

Pseudoletter Heightened Overlapped Handwritten Cheque Segmentation and Forgery Detection Framework Using Sgcip-Cnn in Banking

¹Hitesh Chaitanyaswami, ²Dr.Ashwin Dobariya

¹ Research Scholar, Department of Computer Application,
Marwadi University, Rajkot, India-360001

²Associate professor, Department of Computer Application, Marwadi University, Rajkot, India-360001

Abstract:

Segmentation of handwritten Bank Cheque Images (BCI) helps to extract important details and makes smoother transactions. However, in previous works, overlapped Handwritten Texts (HT) with Printed Texts (PT) are not concentrated, disrupting the segmentation process. Therefore, this framework used Intelligent Character Recognition (ICR) and Pseudo Letter with Height-based Segmentation (PLHS) to effectively remove the overlapped texts for accurate HT segmentation. At first, the BCI is preprocessed to obtain a denoised enhanced image. From the enhanced BCI, the overlapped HT with PTs are recognized and segmented separately using ICR and PHLS. Then, the date, signature, name, and amount from HT are separately identified using Nanonets. After that, the faded texts are redrawn using texture inpainting followed by edge detection and contour formation. Finally, the recognized texts are categorized as forged and genuine cheques using a Sigmoidal Growing Cosine Intermap Pooling-based Convolutional Neural Network (SGCIP-CNN) with a classification accuracy of 98.7899% for effective money transactions. Thus, the proposed work outperformed the existing methodologies.

Keywords: Median Filter (MF), Squeeze Theorem based Contrast Limited Adaptive Histogram Equalization (ST-CLAHE), Sobel Sparse Marr-Hildreth Edge Detector (SSMHED), Handwritten Texts (HT), Forged Cheques (FC), Genuine Cheques (GC), Money Transaction Process (MTP).

1. Introduction

In the realm of financial transactions, handwritten bank cheques play a significant role in facilitating MTP. Despite the proliferation of digital payment methods (Kohli & Kumar, 2021), cheques remain prevalent, particularly in contexts where trust, tradition, and legal requirements converge (Kaur & Kumar, 2023). However, processing these BCI is difficult due to handwriting styles, ink colors, and paper quality (Bogahawatte et al., 2021). Thus, the effective segmentation of handwritten BCI is important for the precise processing (Abdulhussien et al., 2023). The segmentation of handwritten BCI enables the extraction of relevant information for secured and effective financial transactions (Adhikary et al., 2023).

Previous works used Machine Learning (ML) techniques (Kaur & Kumar, 2021), such as Support Vector Machine and Hidden Markov Models (Qaroush et al., 2022) for segmenting the handwritten BCI. Other Deep Learning (DL)

methods, such as Convolutional Neural Network (CNN) and Deep Neural Network (DNN) (Patil et al., 2022) use Optical Character Recognition (OCR) (Ashikur Rahman et al., 2022) that identify HT for segmentations (Optoelectronics, 2023). However, ML and DL methods failed to segment the overlapped HT from the PT, disrupting the segmentation. Therefore, to overcome the issue, the proposed work effectively segmented the overlapped HT for genuine MTP.

1.1 Problem Statement

The issues in previous works are described below,

- None of the works had concentrated on separating the overlapped HT from the PT.
- Previous work did not focus on classifying the GC and FC for effective MTP.
- The noises in the images were not removed in previous works that hindered the segmentation process.

- Handwritten numbers, characters, and signatures were not categorized in (Faizullah et al., 2023), which affected the efficiency of GC identification.
- The handwritten faded text was not concentrated in (Aanchal et al., 2022), which wrongly categorized GC as FC.

The objectives of the proposed work are detailed below,

- HT is effectively separated from PT using ICR and PHLS.
- For GC and FC categorization, SGCIIP-CNN is utilized.
- For obtaining the enhanced BCI, MF and ST-CLAHE are used.
- Handwritten numbers, characters, and signatures are separated using Nanonets for GC identification.
- The faded text in BCI is redrawn using texture inpainting technique.

The rest of the paper is organized as: section 2 discusses the related works, section 3 describes the proposed methodology, section 4 presents the results and discussion, and finally, section 5 concludes the proposed work with future development.

2. Literature Survey

(Faizullah et al., 2023) introduced an effective framework named Arabic Check Courtesy Amount Recognition using segmentation techniques. This technique utilized the segmentation-based and segmentation-free approaches that separated the numbers on the check images for effective segmentation. But, the BCIs were processed without removing the illuminations and shadows that affected the segmentation process.

(Aanchal et al., 2022) developed a framework named automated bank cheque verification system using Leaflet Segmentation (LS). DL-based

CNNs and OCR techniques were utilized for recognizing the HTs. The recognized HTs were segmented effectively using LS for the further verification process. But, in this methodology, the HTs were segmented without redrawing the faded texts that affected the precise segmentation.

(Wei et al., 2021) represented a framework for HT image segmentation in BCI to enhance character recognition accuracy using the CNN technique. Here, HTs in BCI were preprocessed to improve the contrast of BCI for effective character-based segmentation. But, the high error rate in this work resulted in inaccurate interpretation that affected BCI segmentation and verification efficiency.

(Chakraborty et al., 2020) accomplished a hybrid approach for enhancing HT segmentation accuracy using CNN and Bidirectional Long Short-Term Memory (BiLSTM). Here, the line-level segmentation was used to enhance the handwritten BCI for further classifications. But, due to varying handwriting styles, the line-level segmentation used in this methodology led to inaccurate recognition of HTs that affected the MTP.

(Nath et al., 2022) established a Semantic Segmentation Technique (SST) using OCR for recognizing the HTs in BCI. Here, SST segmented HT regions, which are then cropped and fed into traditional OCR engines for effective HT recognition. However, in this methodology, the BCI was segmented without separating the PT from HT, which affected the entire work performance.

3. Proposed Handwritten Cheque Segmentation And Classification Model

In this paper, an effective framework for accurate segmentation of BCI and categorization of GC and FC is proposed for effective MTP. The structural diagram of the proposed work is shown in figure 1,

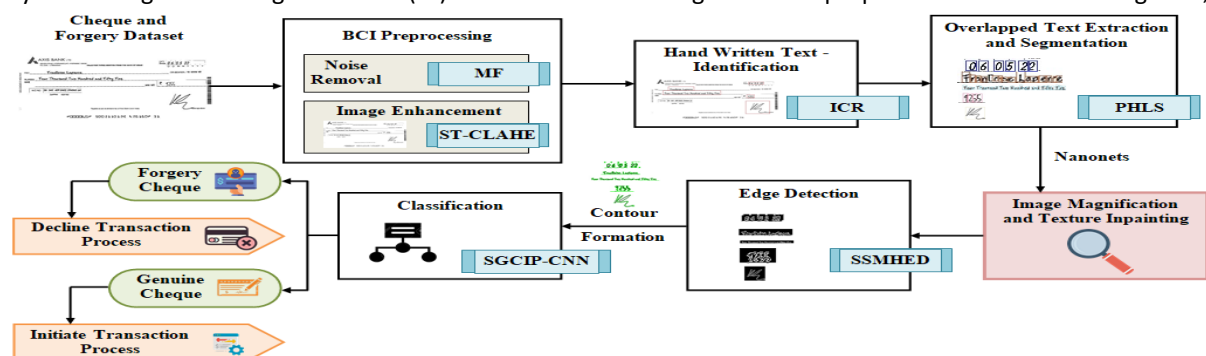


Figure 1: Structural Diagram of the Proposed Work

3.1 Data Collection

The proposed work starts by collecting the BCI from the Cheque Image Dataset (CID) and signatures from the Forgery & Real Signature Dataset (FRSD). The (n) numbers of collected images (I_{cheque}) are expressed as,

$$I_{cheque} = I_1, I_2, \dots, I_n \quad \text{where } cheque = 1 \text{ to } n \quad (1)$$

Then, (I_{cheque}) are pre-processed for further analysis.

3.2 BCI Preprocessing

From (I_{cheque}) , the noises are removed using MF, which replaces each pixel value with the median value of its neighborhood. Thus, the denoised images $(I_{denoised})$ are given as,

$$I_{denoised}(m'', n'') = \left\lfloor \frac{m'' + n''}{2} \right\rfloor \times (I_{cheque}(m'', n'')) \quad (2)$$

Here, (m'', n'') represents the pixels of (I_{cheque}) . After that, the images are enhanced using Contrast Limited Adaptive Histogram Equalization (CLAHE) for clear visualization. CLAHE enhances the $(I_{denoised})$ by using the Histogram Equalization (HE) technique for a more balanced contrast image. But, pixels that exceed the specified clipping limit in CLAHE can result in the loss of subtle image details. Hence, the Squeeze Theorem (ST) is utilized, which mitigates the loss of subtle details caused by clipping.

At first, the $(I_{denoised})$ are divided into non-overlapping regions $(I^{non-overlapping})$ with (\hat{e}) number of pixels. After that, the HE is applied to each $(I^{non-overlapping})$ as,

$$H^E = \frac{E-1}{\hat{e}} \times I^{non-overlapping} \quad (3)$$

Here, (E) represents the maximum intensity level of $(I^{non-overlapping})$ and (H^E) represents the histogram-applied images. Then, the enhanced image $(I^{enhanced})$ is obtained by clipping (H^E) using ST, which prevents information loss in images. This is formulated as,

$$I^{enhanced} = C^{clip} \left(\lim_{I^{non-overlapping} \rightarrow \hat{e}} \times E(H^E) \right) \quad (4)$$

Where, (C^{clip}) represents the clip limit. Thus, $(I^{enhanced})$ is then used for HT analysis.

3.3 Handwritten Text Identification

From $(I^{enhanced})$, the HT is identified automatically using the ICR technique. ICR excels in understanding different handwriting styles, fonts, and handwritten and printed letters. It also identifies the HT by using several features, such as stroke widths, curvature, character heights, spacing, texture patterns, baseline detection, slanted lines, and aspect ratios.

Thus, based on several features, the identified HT images $(I^{identified})$ are represented as,

$$I^{identified} \leftarrow I^{enhanced} (I^{HT}, I^{PT}) \quad (5)$$

Here, (I^{HT}) represents the HT and (I^{PT}) represents the PT. After that, the HT is extracted completely from the overlapped PT for effective segmentation, which is discussed below.

3.4 Overlapped Text Extraction and Segmentation

From $(I^{identified})$, the HT that is overlapped with PT is extracted and segmented using the PHLS technique. This technique combines Pseudo Letter Segmentation (PLS) with height-based analysis for effective segmentation of HT.

- At first, $(I^{identified})$ are segmented letter by letter using the below formula,

$$I^{LS} = I^{segmenting} (I^{identified} (I^{HT} \times I^{PT} (I^{HT}))) \quad (6)$$

Here, (I^{LS}) represents the segmented pseudo letters, $(I^{segmenting})$ represents the segmentation process, and $(I^{PT} (I^{HT}))$ represents the HT that is overlapped with PT. Here, the (I) numbers of (I^{LS}) are given as,

$$I^{LS} = I^1, I^2, \dots, I^l \quad (7)$$

- Then, from each (I^{LS}) , the mean (M^H) and variance (V^H) of heights for HT and PT are calculated as,

$$M^H = \frac{1}{l} \sum_{k=1}^l I_{jk}^{HT} \quad (8)$$

$$V^H = \frac{1}{l} \sum_{j=1}^l (I_j^{HT} - M^H)^2 \quad (9)$$

Here, (I_{jk}^{HT}) represents the height of (j^{th}) pseudo letter with index (k) in a row. Thus, by computing the (M^H) and (V^H) , the heights of HT and PTs are identified and are represented as $(I_{HT-Height}, I_{PT-Height})$. After that, based on $(I_{HT-Height}, I_{PT-Height})$, the HTs are extracted separately as shown below,

$$Q_{extract} = HT \times (I_{HT-Height} - I_{PT-Height}) \quad (10)$$

Here, $(Q_{extract})$ represents the extracted HTs, and from $(Q_{extract})$, the segmented HTs (I_{SEG}) are obtained, which are given as,

$$(I_{SEG} \leftarrow Q_{extract}) \quad (11)$$

Then, (I_{SEG}) are given to Nanonets for further separation process.

3.4.1 Nanonets

From (I_{SEG}) , name (I_{name}) , date (I_{date}) , amount (I_{amount}) , account number $(I_{accountnumber})$, and signature $(I_{signature})$ are separately identified using Nanonets, which is an artificial intelligence based document processing tool. Nanonets are designed to recognize HT efficiently. Its automated functionality distinguishes and extracts (I_{name}) , (I_{date}) , (I_{amount}) , $(I_{accountnumber})$, and $(I_{signature})$ from handwritten cheques for smoother financial transactions. This is formulated as,

$$I_{SEG} \rightarrow I_{NANO}(I_{dates}, I_{amount}, I_{signature}, I_{names}, I_{accountnumber}) \quad (12)$$

Thus, the grouped characters of HT are denoted as (I_{NANO}) .

3.5 Image Magnification and Texture Inpainting

Then, the (I_{NANO}) are enlarged or magnified (I_{MAG}) for clear observation and understanding of intricate structures within the image. After that, the Texture Inpainting (TP) is performed for faded HT by redrawing the faded text. Thus, TP enhances clear texture information by preserving the appearance and coherence of the text. Thus, the clearly appeared HT (I_{CA}) is given as,

$$I_{CA} \leftarrow I_{MAG} \quad (13)$$

Then, the edges are detected for (I_{CA}) , which are described further.

3.6 Edge Detection

From (I_{CA}) , the edges are detected using a Marr-Hildreth Edge Detector (MHED) with Laplacian Operator (LP). But, LP does not represent the thin strokes in HT as it produces thicker edges. Hence, Sobel-based Sparse Representation (SSR) is used, which enhances Edge Detection (ED) in HT by highlighting gradients and refining the ED. Thus, SSR improves the accuracy of identifying thin text strokes efficiently.

→ At first, for input (I_{CA}) , the gradients $(G_{(x)}, G_{(y)})$ in both directions (x, y) are computed using Sobel operators (S_x^O, S_y^O) as,

$$(G_{(x)}) = I_{CA} * S_x^O \quad (14)$$

$$(G_{(y)}) = I_{CA} * S_y^O \quad (15)$$

→ Then, the gradient magnitude $(M(x, y))$ and orientation $(\theta(x, y))$ are calculated using the below formula,

$$M(x, y) = \sqrt{G_{(x)}^2 + G_{(y)}^2} \quad (16)$$

$$\theta(x, y) = \arctan 2(G_{(y)}, G_{(x)}) \quad (17)$$

Here, (\arctan) represents the inverse of the tangent function. After that, the Sparse

Representation (S^{REP}) is applied to enhance the ED by refining the ($G_{(x)}, G_{(y)}$), which is given as,

$$S^{REP}(x, y) = \frac{1}{1 + \alpha \cdot M(x, y)} \quad (18)$$

Here, (α) represents the parameter that controls the enhancement of ($G_{(x)}, G_{(y)}$). Then, by applying the threshold, the edges are accurately detected, which is denoted as (I_{ED}).

Pseudo code of SSMHED

Input: Clearly Appeared HT, (I_{CA})

Output: Edge Detected HT, (I_{ED})

Begin

Initialize iterations, (t, t^{\max})

While ($t < t^{\max}$)

Initialize (I_{CA})

Compute ($G_{(x)}, G_{(y)}$) using

(S_x^o, S_y^o)

Calculate ($M(x, y)$), ($\theta(x, y)$)

problem. Hence, Sigmoidal Growing Cosine Unit (SGCU) and Intermap Pooling (IP) are used. Here, SGCU enhances feature representation, while IP

$$M(x, y) = \sqrt{G_{(x)}^2 + G_{(y)}^2}$$

$$\theta(x, y) = \arctan 2(G_{(y)}, G_{(x)})$$

Apply

$$S^{REP}(x, y) = \frac{1}{1 + \alpha \cdot M(x, y)}$$

End while

Return $\rightarrow (I_{ED})$

End

Then, from (I_{ED}), the contour is formed for effective classification. The contour-formed HT images are represented as (I_{CF}).

3.7 Classification

Finally, from (I_{CF}), the BCI is classified as GC and FC for safe and accurate MTP using CNN. But, the flattening layers in CNN simply convert the 2D or 3D feature maps into a 1D vector without considering the spatial relationships. Thus, CNN potentially loses important structural information; also, it has a slow learning

improves spatial information retention. The SGICIP-CNN classifier is shown in Figure 2,

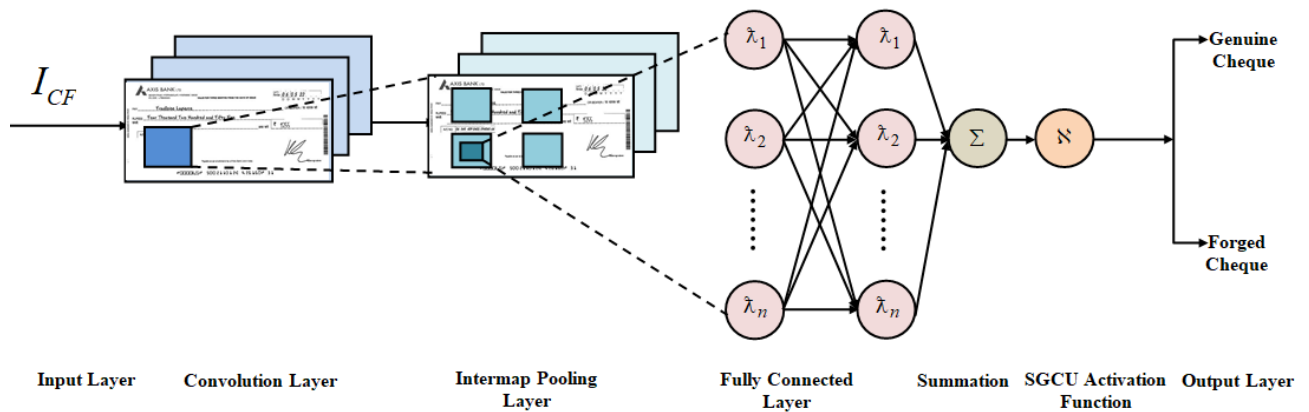


Figure 2: SGICIP-CNN Classifier

The working steps of SGICIP-CNN are detailed below,

Input Layer

Firstly, the (s'') numbers of (I_{CF}) are initialized as,

$$I_{CF} = I_1, I_2, \dots, I_{s''} \quad (19)$$

Convolutional Layer

Then, the input (I_{CF}) is given to the convolutional layer with SGCU activation for a fast learning process. Thus, the convoluted output (Z_{uv}^{CON}) at position (u, v) is given as,

$$Z_{uv}^{CON} = \mathbb{S} \left(\sum_e \sum_f (k'_{ef} \times I_{CF(u+e)(v+f)} + b) \right) \quad (20)$$

Here, (k') represents the kernel function, (e, f) represents the indices used for iterating over the elements of (I_{CF}) and (k') , (b) represents the bias term, and (\mathbb{S}) represents the SGCU activation function. Thus, the (\mathbb{S}) using cos function (\cos) and exponential function (e) is given as,

$$\mathbb{S}(I_{CF}) = \frac{1}{e^{-I_{CF}} (I_{CF} + \cos(I_{CF}))} \quad (21)$$

Intermap Pooling Layer

After convolution, the intermap-pooling operation $(\wp(Z^{CON}))$ is performed, which improves spatial information retention. This is formulated as,

$$\wp(Z^{CON}) = \max_{\gamma \rightarrow -a+1, \dots, 0} \tilde{\wp}(u', v', k', a + \gamma) \quad (22)$$

Here, (γ) represents the (a) number of iterative variables that range from $(-a+1, \dots, 0)$, (\max) represents the maximum function, and $(\tilde{\wp}(u', v', k', a + \gamma)(l))$ represents the value of $(a + \gamma)^{th}$ feature map at spatial location (u', v') within the (k') group of (l^{th}) feature map.

Flattened Layer

The flattened layer converts the multi-dimensional output into a one-dimensional vector. Thus, the flattening (L^{flat}) of output of $(\wp(Z^{CON}))$ is given as,

$$I_{Flat} = L^{flat} \cdot (\wp(Z^{CON})) \quad (23)$$

Here, (I_{Flat}) represents the flattened output.

Fully Connected layer

A Fully Connected Layer (FCL) integrates high-level feature representations from previous layers. Thus, the output of FCL (I^{FCL}) using (I_{Flat}) is expressed as,

$$I^{FCL} = \mathbb{S}(w_{FCL} \cdot I_{Flat} + b_{FCL}) \quad (24)$$

Where, (w_{FCL}, b_{FCL}) represents the weight and bias of a (I^{FCL}) , and (\mathbb{S}) represents the SGCU activation.

Output Layer

Hence, the classifies FC and GC, which are denoted as $(C^{forgery})$ and $(C^{genuine})$, respectively for accurate MTP.

Pseudo code of SGCIIP-CNN

Input: Contour Formed HT Images, (I_{CF})

Output: Forged and Genuine cheques, $(C^{forgery}, C^{genuine})$

Begin

 Initialize iterations (γ, γ^{\max})

 While $(\gamma < \gamma^{\max})$

 Initialize (I_{CF})

 Calculate

$$Z_{uv}^{CON} = \mathbb{S} \left(\sum_e \sum_f (k'_{ef} \times I_{CF(u+e)(v+f)} + b) \right)$$

 Compute intermap-pooling,

$$\wp(Z^{CON}) = \max_{\gamma \rightarrow -a+1, \dots, 0} \tilde{\wp}(u', v', k', a + \gamma)(l)$$

 Evaluate

$$I^{FCL} = \mathbb{S}(w_{FCL} \cdot I_{Flat} + b_{FCL})$$

 End while

 Return $\rightarrow (C^{forgery}, C^{genuine})$

End

Thus, the MTP for $(C^{genuine})$ is initiated, and the MTP for $(C^{forgery})$ is declined for a secured and precise transaction process. The performance assessment of the proposed work is described in further sections.

4. RESULTS AND DISCUSSION

In this section, the proposed work is compared with existing methodologies and related works to evaluate the effectiveness of the proposed model. The entire work is implemented in the PYTHON platform.

4.1 DATASET DESCRIPTION

The proposed work uses two datasets, namely CID and FRSD, which are collected from the Kaggle platform. The CID dataset contains 10000 BCI and FRSD contains 1020 Signature images with 2

classes as forged and genuine. The dataset is described in Table 1,

Table 1: Dataset Description of the proposed work


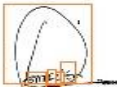


























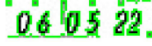




| Datasets | CID | FRSD |
|--------------|-------|------|
| Total Images | 10000 | 1020 |
| Training | 8000 | 816 |
| Testing | 2000 | 204 |

4.2 Performance Analysis of the Proposed Work

Here, the performance of the proposed SGCIP-CNN, PHL5, ST-CLAHE, and SSHMED is compared with traditional techniques. The image results of the proposed work are shown in Table 2,

Table 2: Image Results of the Proposed Work

| BCI SEGMENTATION | | | |
|------------------|--|--|--|
| Input BCI | | | |
| Enhanced BCI | | | |
| HT recognition | | | |
| Segmented texts | | | |

| | | | |
|-------------------|--|---|--|
| |  |  |  |
| Edge Detection |      |      |      |
| Contour formation |      |      |      |

Initially, the input BCIs are enhanced using ST-CLAHE and then recognized using ICR and Nanonets. After that, the recognized HTs are segmented separately as date, name, amount, and

signature using PHLS techniques. Then, the edges are detected and the contour is formed as shown in Table 2. Finally, HT-BCIs are classified as GC and FC for effective MTP. The performance analysis of PHLS is shown in Figure 3,

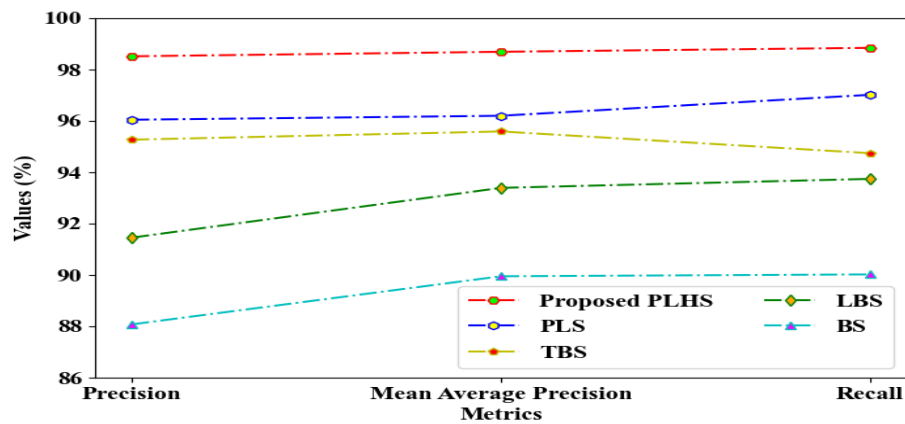


Figure 3: Performance analysis of the proposed PHLS

The performance analysis of the proposed PHLS is compared with traditional PLS, Threshold-Based Segmentation (TBS), Line-Based Segmentation (LBS), and Behavioural Segmentation (BS) techniques as shown in Graph 3. Here, the proposed PHLS accurately extracted the HT that overlapped with PT using height-based techniques,

attaining a higher Mean Average Precision, Precision, and Recall of 98.6925%, 98.5167%, and 98.8456%, respectively. But, when compared to the proposed PHLS, the existing techniques had lower performance, which degraded the overall performance.

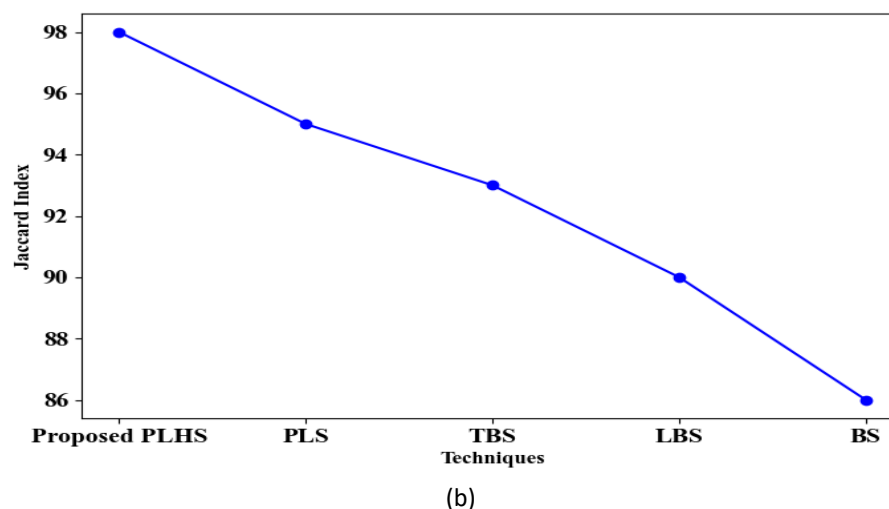
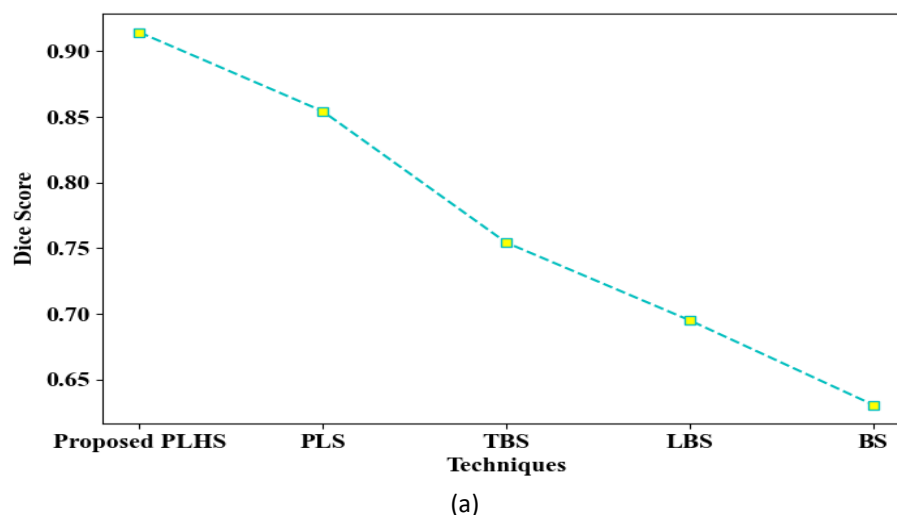
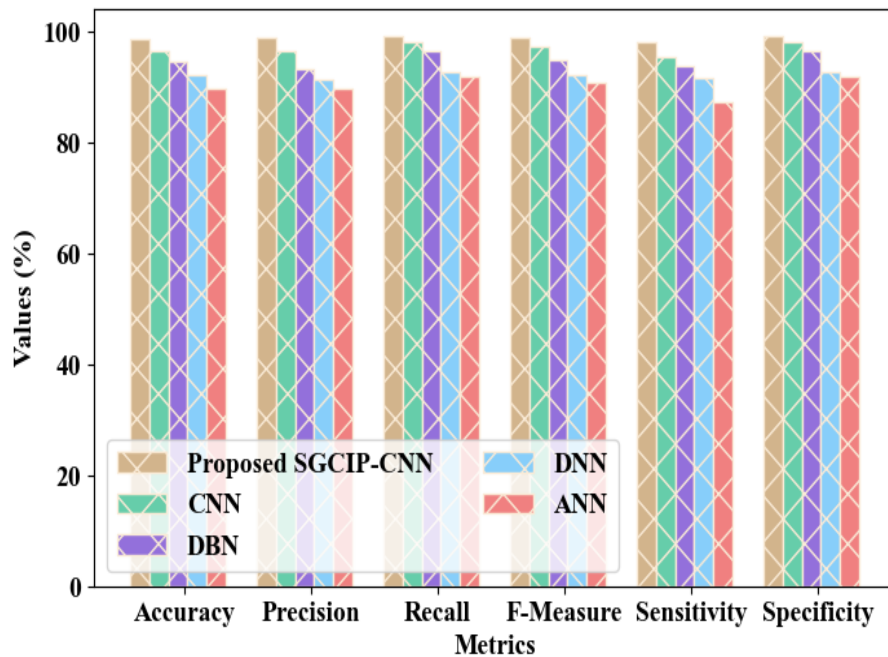


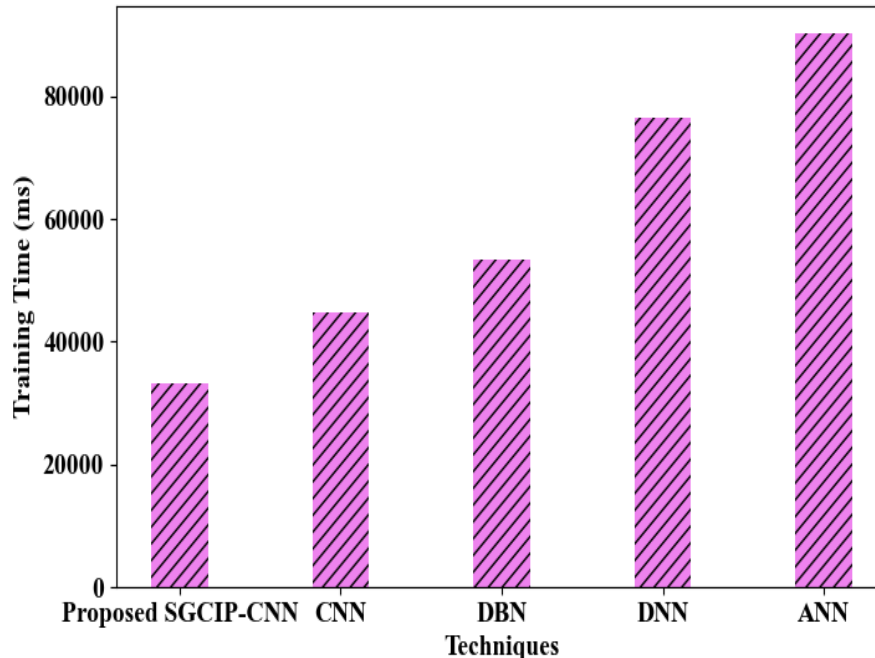
Figure 4: (a) Dice Score (b) Jaccard Index

Figures 4 (a) and (b) describe the Dice Score (DS) and Jaccard Index (JI) of the proposed PHLS and the existing techniques. As shown in Figures 4 (a) and (b), when compared with existing methodologies, the proposed PHLS had higher DS

and JI values of 0.91458 and 0.045128, respectively. The height-based techniques in PHLS enhanced the segmentation process, outperforming the traditional techniques.



(a)



(b)

Figure 5: Performance assessment of the proposed SGCIIP-CNN

The graph in Figures 5 (a) and (b) shows the performance analysis of the proposed SGCIIP-CNN with the Training Time (TT). Here, the proposed

SGCIIP-CNN used IP and SGCU activation for enhanced performance, attaining higher Accuracy, Precision, Recall, F-measure, Specificity, and

Sensitivity of 98.7635%, 98.8361%, 99.1287%, 98.9671%, 98.1921%, and 99.1287%, respectively with the minimum TT of 33243 ms. But, the

existing techniques had a lower performance with maximum TTs that hindered the accurate classification process.

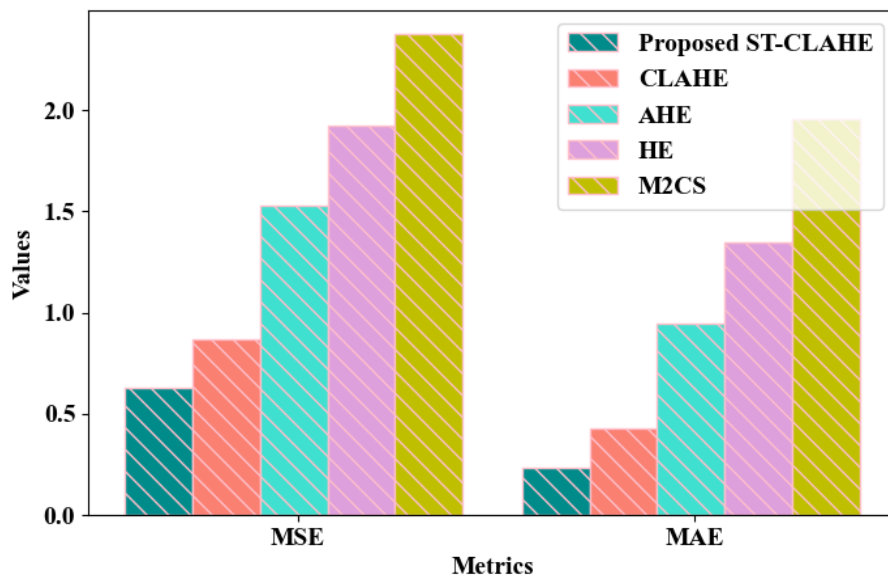


Figure 6: MSE and RMSE validation

Figure 6 describes the Mean Square Error (MSE) and Root Mean Square Error (RMSE) validation of the proposed ST-CLAHE with traditional CLAHE, Adaptive Histogram Equalization (AHE), HE, and Min-Max Contrast Stretching (M2CS). MSE and RMSE evaluate image enhancement by quantifying differences between original and processed

images. Here, when compared with state-of-the-art works, the proposed ST-CLAHE attained minimum MSE and RMSE values of 0.6265 and 0.2318, respectively. Due to the usage of ST in CLAHE, the contrast was enhanced, outperforming the traditional techniques.

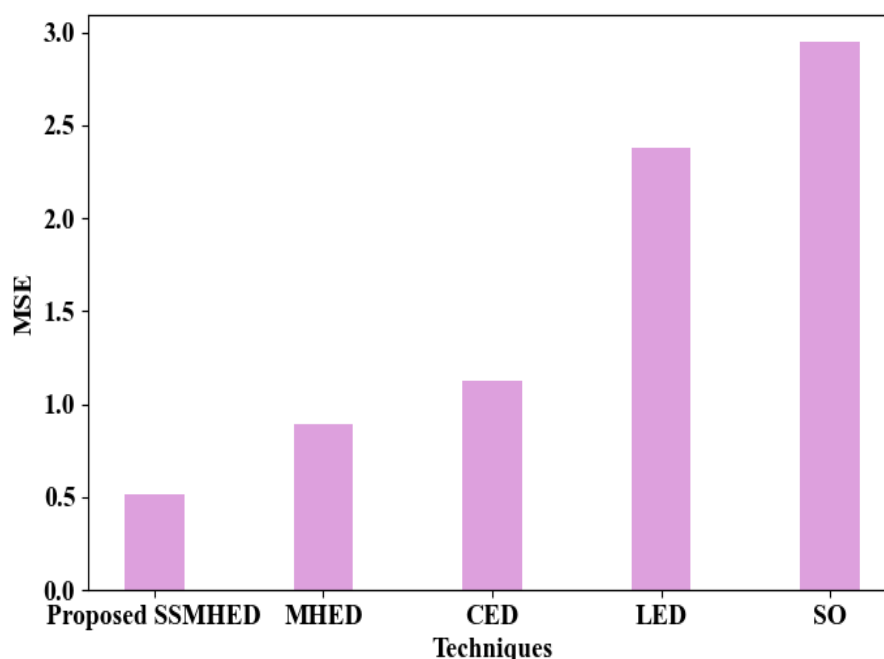


Figure 7: MSE of the proposed SSMHED

The MSE value of the proposed SSMHED is compared with existing HMED, Canny Edge

Detector (CED), Laplacian Edge Detector (LED), and Sobel Operator (SO) as shown in graph 7. Here, the

proposed HMED uses the SSR technique to enhance the ED, attaining a minimum MSE value of 0.5104. But, existing techniques had maximum

MSE values, resulting in inaccurate detection of edges. Thus, the proposed work outperformed the traditional works.

Table 3: Comparative Analysis with Related Works

| Study | Techniques used | Dataset | Accuracy (%) |
|---------------------------|------------------------|------------------------------------|--------------|
| Proposed Work | PHLS | CID | 98.76 |
| (Agrawal et al., 2020) | Word Segmentation | Gurumukhi handwritten word samples | 88.78 |
| (Ahmad, 2023) | Histogram Segmentation | UTSig | 95.58 |
| (Saqib et al., 2022) | Character Segmentation | APTID-MF | 95 |
| (Mahadevkar et al., 2024) | Text-line Segmentation | - | 88 |
| (Pearlsy & Sankar, 2023) | SFF | - | 96.2 |

The proposed work used PHLS segmentation, while the traditional works used Segmentation Facilitate Feature (SFF), word, histogram, character, and text-line segmentation as shown in Table 3. In the proposed PHLS, the height-based techniques are included, which enhance the model's performance. The datasets used in the proposed and existing works are CID, Gurumukhi handwritten word samples, Arabic Printed Text Image Database/Multi-Font (APTID-MF), and University of Tehran Persian Signature (UTSig) datasets. From Table 3, it is shown that the existing works attained a lower average accuracy of 92.71%, while the proposed work attained a higher accuracy of 98.76%, thus outperforming the traditional works.

5. Conclusion

This research proposed a PHLS technique for extracting the overlapped HT with PT for effective segmentation. This method preprocessed the BCI to obtain an enhanced image with minimum MSE and RMSE values of 0.6265 and 0.2318, respectively. After that, the HTs are segmented using the PHLS technique with the highest precision and recall of 98.5167% and 98.8456%, respectively. Then, the edges are detected with the minimum MSE value of 0.5104. Finally, GC and FC are classified using SGCIIP-CNN with a higher accuracy of 98.7635% for effective money transactions.

Future Recommendation

This work segmented and classified GC and FC for effective transactions. But, it did not concentrate

on cheque securities. Hence, in the future, various techniques will be implemented to securely segment the cheques for safer transactions.

REFERENCE

- [1] Aanchal, Nidhi, Preeti, & Gurpratap. (2022). Automatic Cropping of Handwritten Scanned Documents with Object Detection Algorithm. *Procedia Computer Science*, 218(2022), 1733–1741.
<https://doi.org/10.1016/j.procs.2023.01.151>
- [2] Abdulhussien, A. A., Nasrudin, M. F., Darwish, S. M., & Abdi Alkareem Alyasseri, Z. (2023). Feature selection method based on quantum inspired genetic algorithm for Arabic signature verification. *Journal of King Saud University - Computer and Information Sciences*, 35(3), 141–156.
<https://doi.org/10.1016/j.jksuci.2023.02.005>
- [3] Adhikary, P. K., Dadure, P., Saha, P., & Pakray, P. (2023). Dzongkha Handwritten Digit Recognition using Machine Learning Techniques. *Procedia Computer Science*, 218, 2350-2358.
<https://doi.org/10.1016/j.procs.2023.01.210>
- [4] Agrawal, P., Chaudhary, D., & Madaan, V. (2020). Automated bank cheque verification using image. *Multimedia Tools and Applications*, 80, 5319–5350.
- [5] Ahmad, I. (2023). A Hybrid Rule-Based and Machine Learning System for Arabic Check Courtesy Amount Recognition. *Sensors*, 1–22.

- [6] Ashikur Rahman, A. B. M., Hasan, M. B., Ahmed, S., Ahmed, T., Ashmafee, M. H., Kabir, M. R., & Kabir, M. H. (2022). Two Decades of Bengali Handwritten Digit Recognition: A Survey. *IEEE Access*, 10(July), 92597–92632.
<https://doi.org/10.1109/ACCESS.2022.3202893>
- [7] Bogahawatte, A., Isuri Samanmali, L. A. H., Perera, M. K. D., Kavindi, T. M. A., Senaratne, N., & Rupasinghe, P. (2021). Online Digital Cheque Clearance and Verification System using Block Chain. 2021 6th International Conference for Convergence in Technology, I2CT 2021, 1–9.
<https://doi.org/10.1109/I2CT51068.2021.9418132>
- [8] Chakraborty, A., De, R., Malakar, S., Schwenker, F., & Sarkar, R. (2020). Handwritten digit string recognition using deep autoencoder based segmentation and ResNet based recognition approach. *Proceedings - International Conference on Pattern Recognition*, 7737–7742.
<https://doi.org/10.1109/ICPR48806.2021.9412198>
- [9] Faizullah, S., Ayub, M. S., Hussain, S., & Khan, M. A. (2023). A Survey of OCR in Arabic Language: Applications, Techniques, and Challenges. *Applied Sciences (Switzerland)*, 13(7). <https://doi.org/10.3390/app13074584>
- [10] Kaur, H., & Kumar, M. (2021). On the recognition of offline handwritten word using holistic approach and AdaBoost methodology. *Multimedia Tools and Applications*, 80(7), 11155–11175.
<https://doi.org/10.1007/s11042-020-10297-7>
- [11] Kaur, H., & Kumar, M. (2023). Signature identification and verification techniques: state-of-the-art work. *Journal of Ambient Intelligence and Humanized Computing*, 14(2), 1027–1045.
<https://doi.org/10.1007/s12652-021-03356-w>
- [12] Kohli, M., & Kumar, S. (2021). Segmentation of handwritten words into characters. *Multimedia Tools and Applications*, 80(14), 22121–22133.
<https://doi.org/10.1007/s11042-021-10638-0>
- [13] Mahadevkar, S., Patil, S., & Kotecha, K. (2024). Enhancement of handwritten text recognition using AI-based hybrid approach. *MethodsX*, 12, 1–11.
<https://doi.org/10.1016/j.mex.2024.102654>
- [14] Nath, G., Pant, V., Sekseria, A., & Kumar, M. (2022). Isolated OCR For Handwritten Forms : An Application in the Education Domain. In *8th International Conference of Business Analytics and 2022*, 1–7.
- [15] Optoelectronics, S. (2023). Semiconductor Optoelectronics,. 42(1), 1674–1679.
- [16] Pearlsy, P.V., & Sankar, D. (2023). Handwriting-Based Text Line Segmentation from Malayalam Documents. *Applied Sciences (Switzerland)*, 13(17), 1–21.
<https://doi.org/10.3390/app13179712>
- [17] Patil, S., Varadarajan, V., Mahadevkar, S., Athawade, R., Maheshwari, L., Kumbhare, S., Garg, Y., Dharrao, D., Kamat, P., & Kotecha, K. (2022). Enhancing Optical Character Recognition on Images with Mixed Text Using Semantic Segmentation. *Journal of Sensor and Actuator Networks*, 11(4), 1–20.
<https://doi.org/10.3390/jsan11040063>
- [18] Qaroush, A., Awad, A., Modallal, M., & Ziq, M. (2022). Segmentation-based, omnifont printed Arabic character recognition without font identification. *Journal of King Saud University - Computer and Information Sciences*, 34(6), 3025–3039.
<https://doi.org/10.1016/j.jksuci.2020.10.001>
- [19] Saqib, N., Haque, K. F., Yanambaka, V. P., & Abdelgawad, A. (2022). Convolutional-Neural-Network-Based Handwritten Character Recognition: An Approach with Massive Multisource Data. *Algorithms*, 15(4), 1–25. <https://doi.org/10.3390/a15040129>
- [20] Wei, C. S., Wang, S. L., Foo, N. T., & Ramli, D. A. (2021). A CNN based handwritten numeral recognition model for four arithmetic operations. *Procedia Computer Science*, 192, 4416–4424.
<https://doi.org/10.1016/j.procs.2021.09.218>